Scientific Research and Essays Vol. 8(3), pp. 139 -151, 18 January, 2013
Available online at http://www.academicjournals.org/SRE
DOI: 10.5897/SRE12.597
ISSN 1992-2248 ©2013 Academic Journals

Full Length Research Paper

Edge detection via statistical features and automatic thresholding technique

Salim Ben Chaabane*, Mounir Sayadi and Farhat Fnaiech

SICISI Unit, ESSTT, 5 Av. Taha Hussein, 1008, Tunis, Tunisia.

Accepted 21 December, 2012

In this paper, the problem of edge detection is addressed using the first order statistics and automatic thresholding technique. The general idea of edge detection using the simple edge detectors such as gradient operators or second derivative operators is extended to the statistic domain. The statistical features are used to describe the relationship between the current pixel and its neighboring, then, the thresholding technique is employed to determine the edge of gray level image. The proposed method improves the accuracy of the edge detection and suppresses the impact of the noise on the results, while the edge has a good consistency. The proposed method is validated by performing a comparative study with respect to other existing techniques. The experimental segmentation results, on standard and textured images, highlight the effectiveness of the proposed method.

Key words: Thresholding, statistical features, first order statistics, noise, segmentation, edge detection, defect detection.

INTRODUCTION

Image segmentation plays an important role in image analysis and computer vision (Shih and Cheng, 2005) (Rodriguez and Suarez, 2006). It is a critical and essential component of an image analysis and/pattern recognition system, and is one of the most difficult tasks in image processing, which determines the quality of the final segmentation (Hun et al., 2011; Grau et al., 2004). The goal of image segmentation is the partition of an image into meaningful or spatially coherent regions sharing similar attributes, such as intensity, color, tone or texture, etc (Yang et al., 2005). Many different techniques of image segmentation have been developed and detailed in the literature (Ben Chaabane et al., 2010). At our knowledge, until, now there is no general technique which can solve all image segmentation types.

Generally, image segmentation approaches are based on either discontinuity and/or homogeneity of information values in a region. The approach based on discontinuity (Davis, 1975), tends to partition an image by detecting isolated points, lines and edges based on abrupt changes in gray levels. However, it is quite important to effectively determine a threshold value for a gray-level image when extracting the edges, that is, to extract objects of interest from their background. The optimal threshold can be readily selected by the entropic thresholding technique (Fan et al., 1996, 1997).

The approaches based on homogeneity (Ben Chaabane et al., 2010), include thresholding, clustering, region growing, and region splitting and merging, etc. Many techniques have been proposed and studied in the last decades to solve the edge detection problem (Nalwa and Binford, 1986; Qian and Huang, 1996; Jianping et al., 2001). These techniques detect the fast change between two regions (Davis, 1975; Nalwa and Binford, 1986). Edge detectors used in these techniques are based on simple gradient operators (Prewiitt, 1970), or second derivative operators (Hildreth, 1980). However, these operators are less sensitive to noise. Consequently, the resulting edges are discontinuous or missed with false edges detection.

Therefore, some post-procedures and pre-processing methods, such as edge tracking, gap filling, smoothing, and thinning, should be applied to obtain the closed

*Corresponding author. E-mail: ben_chaabane_salim@yahoo.fr.

region boundaries and to reduce the influence of undesired factors such as noise. All these post-procedures are time-consuming and thus, the edge detection becomes a tedious task. Notice that, the actual region boundaries should be closed curves.

To overcome all these disadvantages, edge detection using statistical features and the automatic thresholding method which avoid the use of pre- and post-processing additional methods is an appearing procedure to be applied.

This paper proposes a hybrid image segmentation technique by integrating the first order statistical features and automatic thresholding technique. After the determination of the local maximum edge strength in the representative feature images, the thresholding technique is used to automatically determine the optimal threshold, that is, to find the region boundaries. This technique allows obtaining a good consistency edges and suppress the impact of the noise on the obtained results. Hence, it can be used to locate the defects in textured images (Mery and Berti, 2002; Nacereddine et al., 2005; Ben Mhammed et al., 2012).

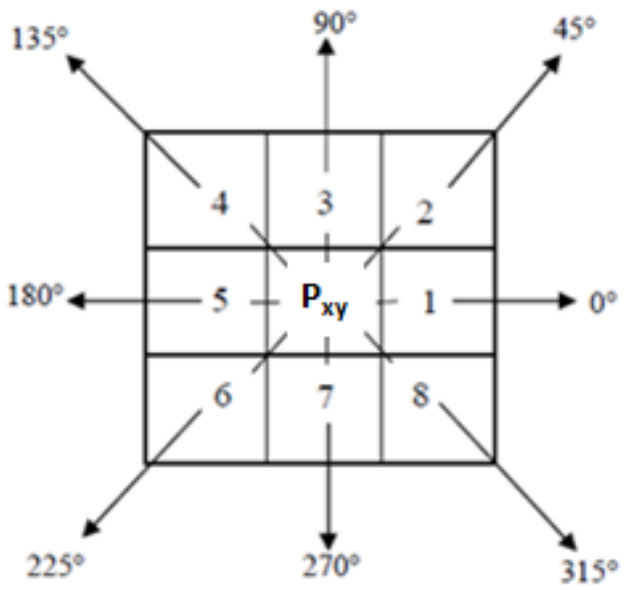

Figure 1. Spatial relationship between pixel p_{xy} at the location (x, y) and its neighbours in the bloc w_{xy} with different angular θ. Here, the neighboring distance $d = 1$ and $\theta = \{0^{\circ}, 45^{\circ}, 90^{\circ}, 135^{\circ}, 180^{\circ}, 225^{\circ}, 270^{\circ}, 315^{\circ}\}$. P_{xy}.

PROPOSED METHOD

Image segmentation based on discontinuity uses the assumption that pixel values change abruptly at the boundary between two regions. Edge detectors used in these segmentation techniques can be divided into two categories: 1) gradient operators and 2) second derivative operators. Gradient operators, such as the Roberts, Prewitt, and Sobel operators (Prewitt, 1970; Davis, 1975), detect the edges by looking for the maximum and minimum in the first derivative of the image luminance. The second derivative operators, such as the Marr-Hildreth and Marr-Poggio operators (Hildreth, 1980; Poggio, 1979), search for zero-crossings in the second derivative of the image luminance to find the edges. However, the obtained edges by these techniques are normally discontinuous or over-detected. In this context, edge detection in the gray level image using statistical features and the thresholding technique appears to be an interesting method. However, to detect the edge in an image using statistical features images and thresholding technique, the determination of the most relevant and representative statistical features plays a crucial role, since assignation of a pixel to classes: edge pixels or non-edge pixels is given directly by the thresholding technique applied to attribute images. In the present study, the representative statistical features are selected by the characterization degree (Van et al., 1999), and the attribute images are computed on overlapping small windows centered on the pixel to be classified. However, the concept of image features was defined to express the image properties relating to the first order statistics. Once the local maximum edge strengths of the attribute images are extracted, the automatic thresholding technique is applied to obtain the final classification pixels.

Edge detection

The task of the edge extraction consists classification of the pixels into two opposite classes: edge versus non edge. However, in an image processing system an image or its derivatives can be represented in various feature spaces. An image can be represented in terms of pixels, which are associated with a location and a gray level value. It can also be represented by its derivatives, e.g., regions with features like average grayscale value, standard deviation, variance, entropy, third order moment, gradient, etc. (Haralick et al., 1973). Features for clustering can be extracted from regions masked by a window $(t \times t)$. By applying thresholding technique, the edge of an image can be found.

In our study, the statistical features are used to describe the relationship between the current pixel (x, y) and its neighboring.

However, a final value of each pixel can be regarded as an angle-related function that contains the spatial information among neighboring pixels.

In Figure 1, eight neighboring pixels of distance one are angularly related to pixel p_{xy} at the location (x, y) in the window w_{xy}.

The statistical features are computed from a sliding window centered around each pixel of the $(M \times N)$ original image (Figure 2). The spatial scanning order of an image is performed, as shown in Figure 3, pixel by pixel from left to right and top to bottom.

This technique is used to calculate the new image called the attribute image (I'). Figures 4(b), (c) and (d), denote the standard deviation image, the variance image and the skewness image, respectively.

However, several attributes can be extracted from the original image. In order to obtain ideal classification pixels, it is necessary to select the most relevant and representative statistical features.

To do this, the characterization degree (Van et al., 1999), is applied to the data set shown in Figure 6. This criterion is based on the computation of the value matrix trace of the variance of interclass pixels divided by the variance of intraclass pixels.

Assume $y_{k_1}^{n_1}$ is the n_1^{th} feature vector estimated for the k_1^{th} image class $(1 \le k_1 \le 12,\ 1 \le n_1 \le 100)$, k_1 is the number of images

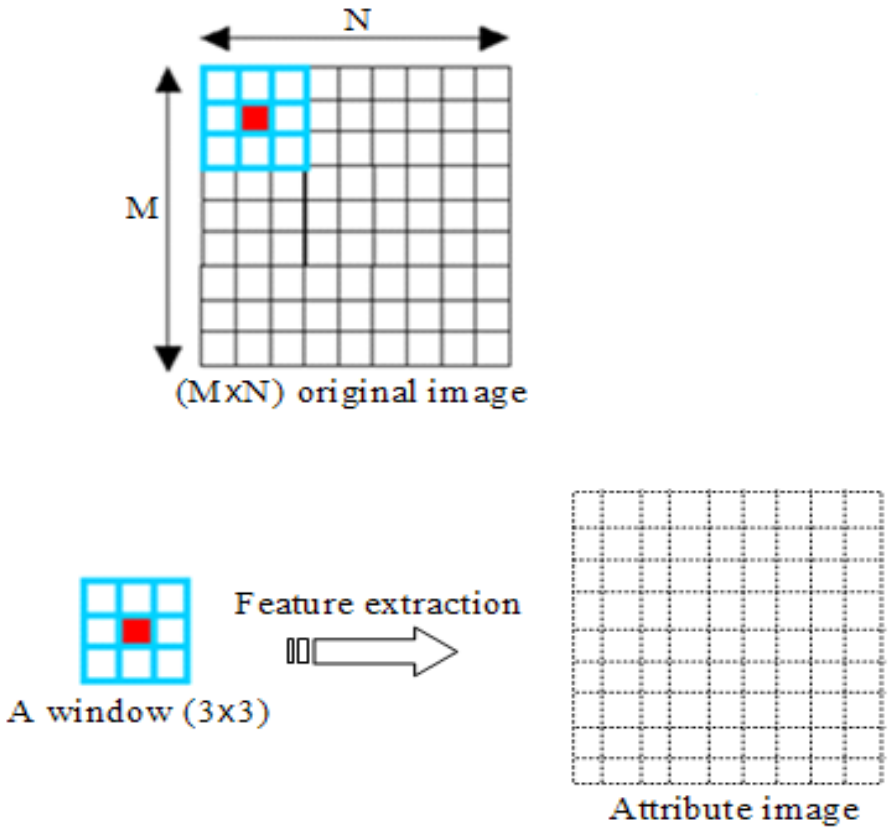

Figure 2. Determination of the attribute (that is, feature) images, using a sliding window.

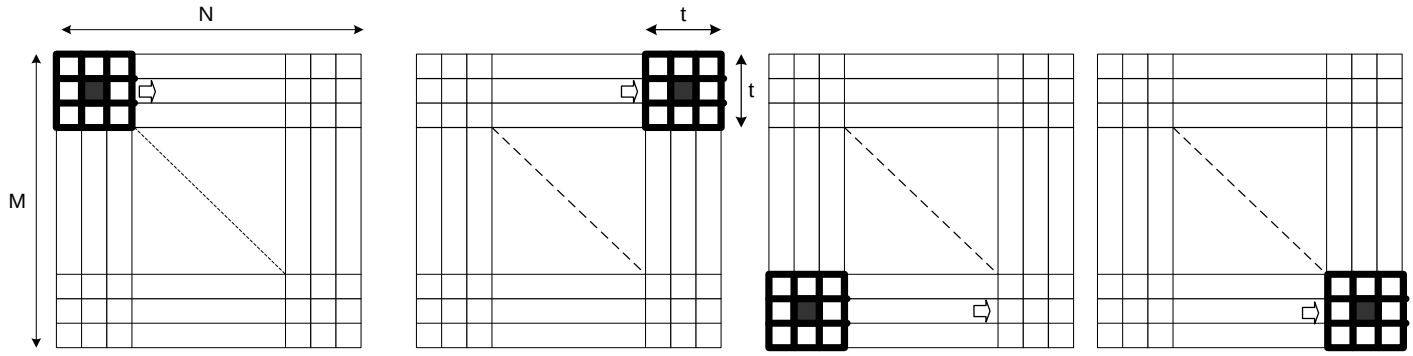

Figure 3. The adaptive sliding window from left to right and top to bottom on an ($M \times N$) image.

and n_1 is the imagettes number of each image. Here, a sub-image denotes a small image belonging to the entire-image.

The mean of the feature vectors m_{k_1} is calculated for the k_1^{th} image class as follow:

$$m_{k_1} = \frac{1}{100}\sum_{k_1=1}^{100} y_{k_1}^{n_1} \quad (1)$$

and the total mean of the features vectors m_c is determined as follow:

$$m_c = \frac{1}{12}\sum_{k_1=1}^{12} m_{k_1} \quad (2)$$

The mean of the intraclass dispersion matrices which represent the maximum likelihood estimation of the covariance matrix of the class, is given by the matrix:

$$S_{intra} = \frac{1}{1200}\sum_{k_1=1}^{12}\sum_{n_1=1}^{100}\left(y_{k_1}^{n_1} - m_{k_1}\right)\left(y_{k_1}^{n_1} - m_{k_1}\right)^t \quad (3)$$

whereas, the mean of the between (inter-class) dispersion matrices

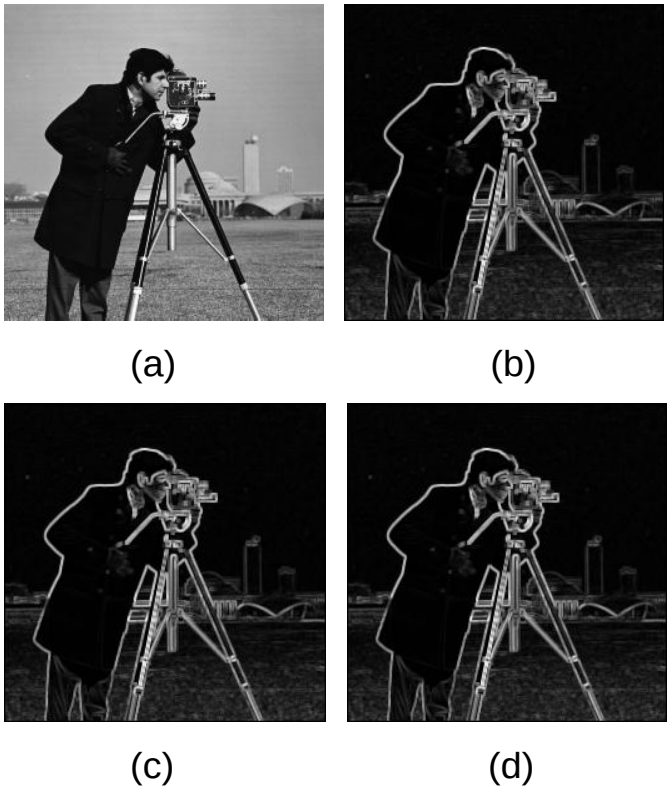

Figure 4. Attribute images of image "Cameraman", (a) standard deviation image, (b) variance image, (c) skewness image.

which describes the scattering of the class sample means is computed using:

$$S_{inter} = \frac{1}{12}\sum_{k_1=1}^{12}(m_{k_1} - m_c)(m_{k_1} - m_c)^t \quad (4)$$

Consequently, the characterization degree $(\mathcal{J})$ is the ration of the between classes (inter-class) variance by the intra-class variance defined by:

$$\mathcal{J} = \text{trace}\,(S_{intra}^{-1}.S_{inter}) \quad (5)$$

Note that the greater the characterization index the better the classification. Referring to the characterization degree plots given in Figure 5, one can observe that the most relevant and representative statistical features are, the variance (Var), the standard deviation (Stan) and the third order moment (Skew).

Assume $g(x,y)$ is the intensity of a pixel $p(x,y)$ at the location (x,y) in an $(M \times N)$ image, designed by (I), w_{xy} is a size $(t_1 \times t_1)$ window centred at pixel $p(x,y)$. The 3 features (Haralick et al., 1973), extracted from the sliding window centred w_{xy} of a pixel $p(x,y)$ at the location (x,y) are given by the following equations:

$$\text{Var}(x,y) = \frac{1}{t_1 \times t_1}\sum_{k=-\frac{t_1-1}{2}}^{\frac{t_1-1}{2}}\sum_{l=-\frac{t_1-1}{2}}^{\frac{t_1-1}{2}}(g(k+x,l+y) - \text{Mean}(x,y))^2 \quad (6)$$

$$\text{Stan}(x,y) = (\text{Var}(x,y))^{\frac{1}{2}} \quad (7)$$

$$\text{Skew}(x,y) = \frac{1}{t_1 \times t_1}\sum_{k=-\frac{t_1-1}{2}}^{\frac{t_1-1}{2}}\sum_{l=-\frac{t_1-1}{2}}^{\frac{t_1-1}{2}}(g(k+x,l+y) - \text{Mean}(x,y))^3 \quad (8)$$

where $(t_1 \times t_1)$ and $g(x,y)$ are respectively the size of the sliding window and the gray scale value of pixel $p(x,y)$, $\frac{t_1+1}{2} \le x \le M - \frac{t_1-1}{2}$ and $\frac{t_1+1}{2} \le y \le N - \frac{t_1-1}{2}$.

$\text{Mean}(x,y)$ is the mean of the gray levels within window w_{xy} and is defined by:

$$\text{Mean}(x,y) = \frac{1}{t_1 \times t_1}\sum_{k=-\frac{t_1-1}{2}}^{\frac{t_1-1}{2}}\sum_{l=-\frac{t_1-1}{2}}^{\frac{t_1-1}{2}}g(k+x,l+y) \quad (9)$$

Note that t_1 must have an odd value to obtain a centered window around each pixel. The gray level image is defined as a two-dimensional $(2-D)$ light-intensity function $g(x,y)$, which contains $(M \times N)$ pixels, each with a value of brightness, that is, grey level, from 0 to N_g. Grey level 0 is the darkest and grey level N_g is the brightest.

Given an optimal threshold T, the input image can be divided into two opposite classes, where the first class consists of grey levels from 0 to T, in such case each gray level is set to 0. The second class contains the other gray levels with $T+1$ to N_g, in that case,

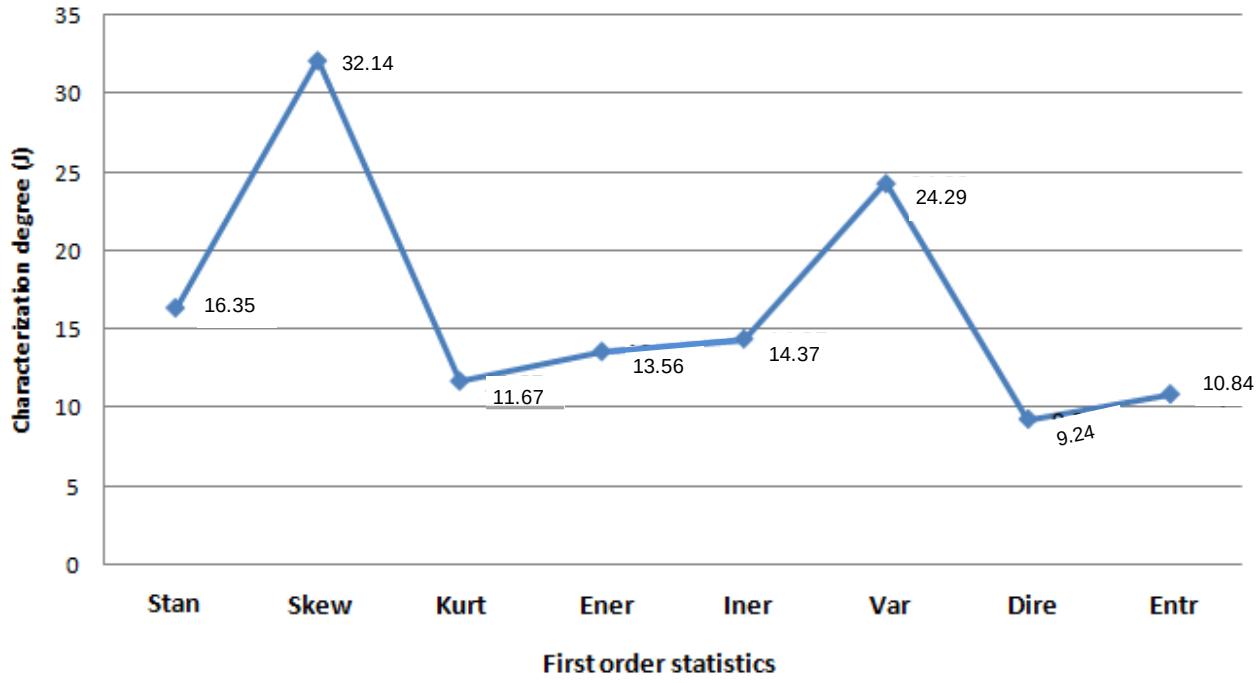

Figure 5. Plot of characterization degree for different statistical features.

each grey level is classified as an edge pixel and is set to 1.

Once the attribute images are formed, their edge strengths are determined using the relationship between the current pixel and its neighboring pixels, as shown in Figure 6(a).

For pixel $p(x,y)$ at the location (x,y), the edge strength is calculated in the four representative patterns, as shown in Figure 6(b).

These edge strengths called the horizontal (ESH), vertical (ESV), northeast diagonal (ESE) and northwest diagonal (ESW) edge patterns are computed as a weighted sum of the pixel values in $R(x,y)$, where the weight coefficients are given in Figure 6(b). Figure 7 shows the edge strengths introduced by these different edge patterns.

For pixel $p(x,y)$ at the location (x,y), the edge strength induced by the horizontal (ESH), vertical (ESV), northeast diagonal (ESE), and northwest diagonal (ESW) edge patterns, are defined respectively by:

$$\begin{aligned} ESH(x,y) = {} & I'(x-1,y-1) + I'(x-1,y) \\ & + I'(x-1,y+1) - I'(x+1,y-1) \\ & - I'(x+1,y) + (x+1,y+1) \end{aligned} \quad (10)$$

$$\begin{aligned} ESV(x,y) = {} & I'(x-1,y-1) - I'(x-1,y+1) \\ & + I'(x,y-1) - I'(x,y+1) \\ & + I'(x+1,y-1) - I'(x+1,y+1) \end{aligned} \quad (11)$$

$$\begin{aligned} ESE(x,y) = {} & I'(x-1,y-1) + I'(x-1,y) \\ & + I'(x,y-1) - I'(x,y+1) \\ & - I'(x+1,y) - I'(x+1,y+1) \end{aligned} \quad (12)$$

$$\begin{aligned} ESW(x,y) = {} & I'(x-1,y) + I'(x-1,y+1) \\ & + I'(x,y+1) - I'(x,y-1) \\ & - I'(x+1,y-1) - I'(x+1,y) \end{aligned} \quad (13)$$

where $I'(x-1,y-1)$ indicates the attribute value of the pixel at $(x-1,y-1)$.

The local maximum edge strength of pixel (x,y), $LMET(x,y)$ is defined as the maximum of the four edge strengths:

$$LMES(x,y) = \max\{ESH(x,y),\ ESV(x,y),\ ESE(x,y),\ ESW(x,y)\} \quad (14)$$

Given an optimal threshold, e.g, T, the E_{LMES} function classifies the pixel on the local maximum edge strength $(LMES)$ in the attribute image into two opposite classes: edge pixels versus non edge pixels (Figure 8), as

$$E_{LMES}(x,y) = \begin{cases} 1, & \text{edge pixel} \quad \text{if } LMES(x,y) \geq T \\ 0, & \text{nonedge pixel} \quad \text{if } LMES(x,y) < T \end{cases} \quad (15)$$

The optimal threshold T is automatically determined by the fast entropic thresholding technique, as described next. In fact the pixel (x,y) is classified as an edge pixel if its local maximum edge strength of the attribute image (LMI) is higher than the optimal threshold determined automatically by the fast entropic thresholding technique, in which case is set to 1. Otherwise, it is classified as a non edge pixel and is set to 0.

Entropic thresholding technique

The optimal threshold can either be selected by the entropic thresholding technique (Fan, 1996, 1997). The technique is

(x-1,y-1)	(x-1,y)	(x-1,y+1)
(x,y-1)	(x,y)	(x,y+1)
(x+1,y-1)	(x+1,y)	(x+1,y+1)

(a)

1	1	1	1	0	-1	1	1	0	0	1	1
0	0	0	1	0	-1	1	0	-1	-1	0	1
-1	-1	-1	1	0	-1	0	-1	-1	-1	-1	0

(b)

Figure 6. (a) First-order neighborhood $R(x,y)$ of current pixel (x,y), (b) weight coefficients for calculating the ESH, ESV, ESE and ESW edge strengths of potential edge patterns.

(a) (b) (c)

(d) (e) (f)

Figure 7. Edge strengths performance based on image “Cameraman”, (a) original image, (b) variance image, (c) edge strength induced by the horizontal edge patterns, (d) edge strength induced by the vertical edge patterns, (e) edge strength induced by the northeast edge patterns, (f) edge strength by the northwest edge patterns.

(a) (b) (c)

Figure 8. Edge detection on image "Cameraman", (a) original image, (b) the local maximum edge strength (c) edges detection obtained by the proposed technique.

shown to be highly efficient for the two-class data classification problem. To illustrate, let the local maximum edge strength of pixels have range $[0, L]$. In an input image, assume that there are f_i pixels whose local maximum edge strength has the value i, $i \in [0, L]$.

If an image can be divided into two classes, edge and non edge classes, by a threshold at level t, where edge class consists of the local maximum edge strength features from 0 to t, and non edge contains the other local maximum edge strength features with $t+1$ to L, then the probability distributions for the edge and non edge pixel classes can be defined, respectively.

Since they are considered as independent distributions, the probability for the nonedge pixels $P_n(i)$ can be defined as:

$$P_n(i) = \frac{f_i}{N_n}, \quad 0 \le i \le t \qquad (16)$$

where $N_n = \sum_{k=0}^{t} f_k$ indicates the total number of pixels that have the local maximum edge strength features in range $0 \le i \le t$.

The probability for the edge pixels can also be calculated by:

$$P_e(i) = \frac{f_i}{N_e}, \quad t+1 \le i \le L \qquad (17)$$

where $N_e = \sum_{k=t+1}^{L} f_k$ indicates the total number of pixels that have the local maximum edge strength features in the range $t+1 \le i \le L$.

The entropies $(E_n \text{ and } E_e)$ for these two pixel classes, respectively, are given by:

$$E_n(t) = -\sum_{i=0}^{t} P_n(i) \log P_n(i) \qquad (18)$$

$$E_e(t) = -\sum_{i=t+1}^{L} P_e(i) \log P_e(i) \qquad (19)$$

The optimal threshold T is selected for performing the non edge and pixel classification has to satisfy the following criterion functions:

$$E(T) = \max_{T=0,1,2,\ldots,L} \{E_n(t) + E_e(t)\} \qquad (20)$$

where E is the total entropy.

As a result, an optimal bi-level threshold can be readily selected by the entropy thresholding technique by maximizing the entropy of the two classes. The major steps of the proposed detector are shown in the flowchart of Figure 10.

EXPERIMENTAL RESULTS AND DISCUSSION

Here, a large variety of gray level images is employed in our experiments (Figure 13). Some experimental results are shown in Figures 9 to 15.

The images originally take 8 bits and have the intensity range from 0 to 255. To evaluate the efficiency and accuracy of the proposed edge extraction method, the results are compared versus existing methods, as described earlier. The efficiency evaluation of these different methods is carried out using computer software.

The proposed edge detection results on textured images to locate the defects (Chao and Tsai, 2008; Liu and Haralick, 2000), (which is a challenging problem in this field), are recorded.

Consequently, standard images (the first three images shown in Figure 13) are developed and used for the numerical evaluation purpose.

First the edge detection results using the proposed method to original image are presented. Figure 9(a) gives the $(N \times M)$ original image of "Lena", where a "saltandpepper" noise of D density was added. This affects approximately $(D \times (N \times M))$ pixels. Figure 9(b) shows the standard deviation image. Figure 9(c) gives the local maximum edge strengths.

The results obtained by the Prewitt, Canny, Sobel and Laplacian edge detectors are given in Figures 9(d), 9(e), 9(f) and 9(g), respectively.

Figure 9(h) shows the extracted edges by performing

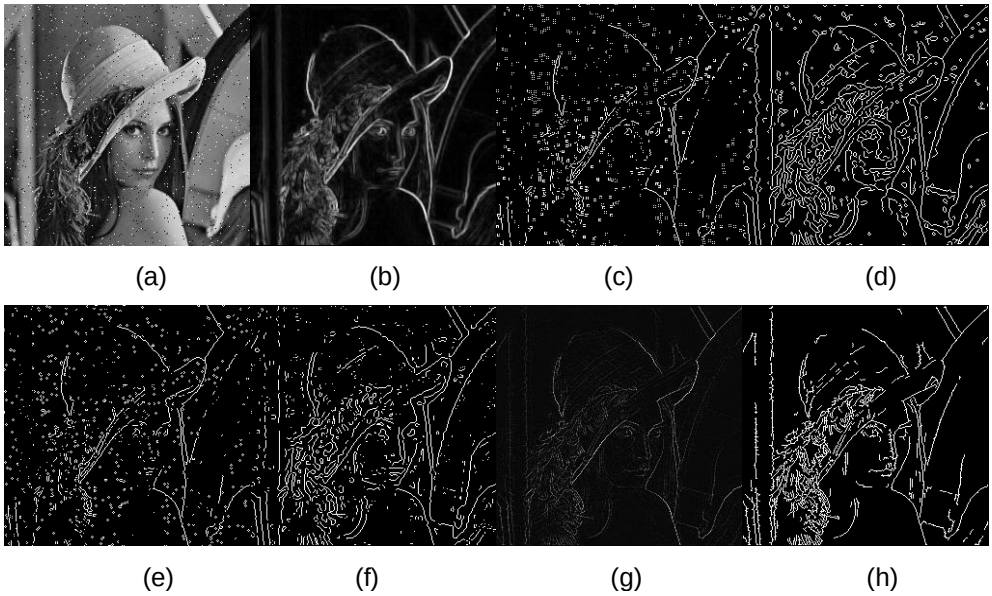

Figure 9. Edge detection performance based on image "Lena", (a) original image disturbed with a "salt & pepper" noise, (b) standard deviation image, (c) detection of the local maximum edge strength in the attribute image, (d) edges obtained by the Prewitt operator, (e) edges obtained by the Canny operator, (f) edges obtained by the Sobel operator, (g) edges obtained by the Laplacian operator, and (h) edges detection obtained by the proposed technique.

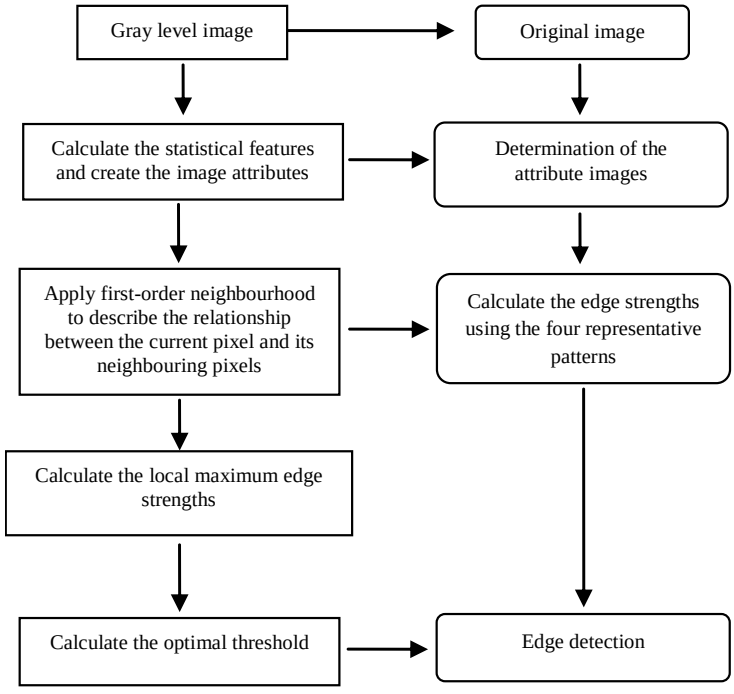

Figure 10. Flowchart of the proposed method.

our edge detector on the standard deviation image. In fact, some obvious edges in the image are missed and some incorrectly classified pixels are presented if only the simple edges detectors are performed on the noisy image. Notice that our edge detector can provide more potential edges as compared with these other detectors

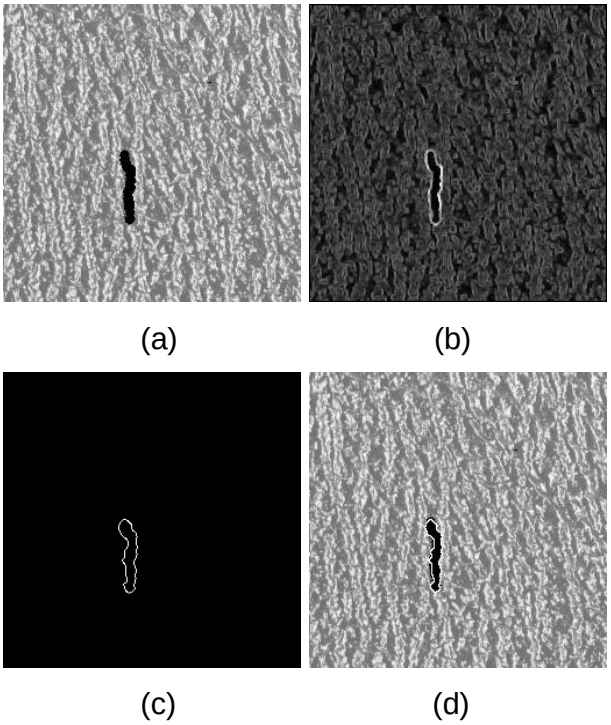

Figure 11. Edge detection and defect localization, (a) original image, (b) deviation standard image, (c) edge detection obtained by our technique, (d) defect localization obtained by our technique.

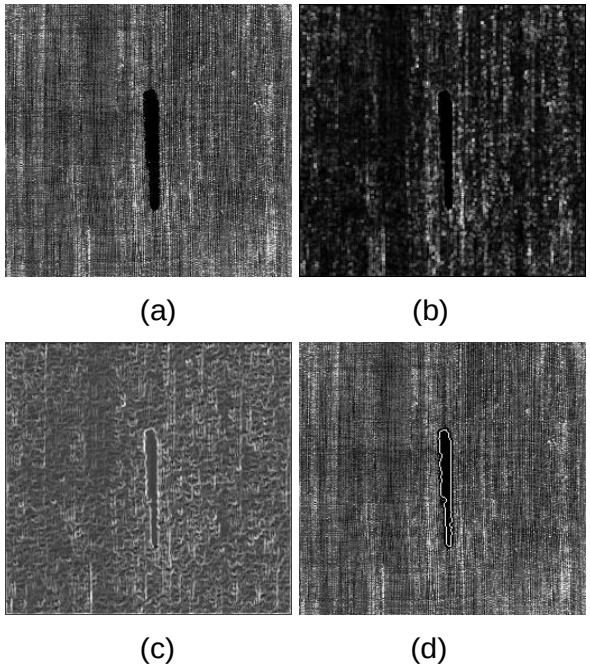

Figure 12. Edge detection and defect localization, (a) original image, (b) variance image, (c) local maximum edge strength, (d) defect localization obtained by our technique.

under the same conditions.

Accordingly, the experimental results indicate that the proposed edge detector can provide more accurate results (Figure 9(h)).

Figure 11(a) shows a textured image with a defect. A sliding window is used to describe the relationship between the current pixel and its neighboring pixels. The resulting image using Equation (1) is given in Figure 11(b). As seen in Figure 11(b), this technique enhances the signal at locations corresponding to the defects.

Since the attribute image, returns the standard deviation of each sliding window, that is, producing the second moment of the sample about its mean, both light and dark edges are equally detected (Ben Mhammed et al., 2012). In Figure 11(d), the thresholding operation is used to define the location of signals corresponding to the defect.

Similarly, detection defect result in the textured image is reproduced in Figure 12. In this case, the attribute image is computed from a sliding window centered on each pixel of the original image by using Equation (2). The obtained image is given in Figure 12(b).

The defect localization can also be observed in Figure 12(d). It can be seen from the resulting image, the defect in the test image which is detected using the local maximum edge strength in the attribute images and the thresholding technique. Therefore, the proposed technique can provide more potential edges as compared with other detectors under the same conditions.

Consequently, the proposed method can be used to segment the location of signal corresponding to the defect, due to consideration of the local information and in the calculation of edge strength of each pixel which is computed as a weighted sum of the pixel values in the four representative patterns, as shown in Figure 6(b).

In order to evaluate the overall performance of the proposed edge detection algorithm versus the conventional edge detection operators, a substantial experiment is then performed.

Regarding the accuracy, Table 1 lists the correct classification rate of the different methods for the data set used in the experiment.

The correct classification rate (Duda et al., 2000; Colot et al., 1998) can be calculated as follows:

$$CCR = \frac{N_{pcc}}{N_{pgt}} \times 100 \qquad (21)$$

with: CCR, N_{pcc} and N_{pgt} denote the correct classification rate (%), the number of correctly classified pixels and the number of the edge pixels in the ground truth images, respectively.

For the accuracy evaluations, the correct classification rate (CCR) method is adopted, but it is only limited in our application to the case of bi-level threshold (M=2) evaluation.

Table 1. Correct classification rate from the Prewitt, Canny, Sobel, Laplacian operators, and the proposed technique for the data set shown in Figure 13.

Classification	Correct classification rate (%)				
	Prewitt operator	Canny operator	Sobel operator	Laplacian operator	Proposed technique
Image 1	90.5685	92.1387	90.3503	88.4109	95.7490
Image 2	90.0772	93.7042	90.1855	89.0640	96.4563
Image 3	92.7765	97.2931	92.6315	92.2577	97.1474

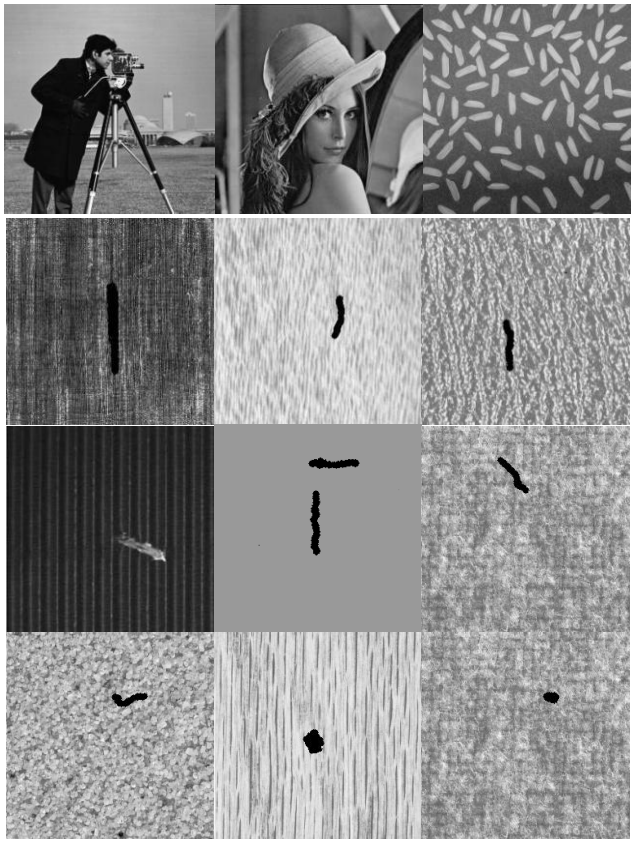

Figure 13. Data set used in the experiment. Twelve were selected for a comparison study. The patterns are numbered from 1 through 12, starting at the upper left-hand corner.

The evaluated natural gray level images with 50 test images, and gray level images extracted from the database of textured images with 100 test images, were used; one sample image is shown in Figure 14 with the corresponding ground truth image.

Acquisition of the correct classified pixels is not a manual process; hence software based on a ground truth image is run. It consists of a small program which compares the labels of the obtained edge pixels and the reference edge pixels as shown in Figure 14(d).

The correctly classified pixel denotes a pixel with a label equal to its corresponding pixel in the ground truth image.

The labelling of the original image is generated by the user based on the used image for segmentation (Figure 14(d)).

The average results for 50 natural test images and 100 test images of the textured database were used to evaluate the accuracy of edge detection for the five methods.

Figures 15(c), 15(d), 15(e), 15(f) and 15(g) show other segmentation results and were obtained using Prewitt, Canny, Sobel, Laplacian operators, and the proposed technique, as used for the edge extraction in the input gray level image.

From these results one can clearly see that the new method allows the enhancement and sharpening of different details of the defects without affecting the background or the neighboring regions.

In fact, the experimental results indicate that the proposed method, which uses the statistical features for local edge strengths calculation, is more accurate than the traditional methods in terms of segmentation quality as denoted by the correct classification rate (Table 1).

Another evaluation criterion is used to measure quantitatively the detection quality of the signal corresponding to the defect. This criterion is based on the determination of the correct and false detection probabilities. In this case, reference edge pixels are necessary (Figure 14(d)). This criterion resides in the comparison between the labels of the obtained edge pixels and the reference edge pixels. In the case where two objects are presented in the reference image R (Figure 14(d)), $R = R_1 \cup R_2$, the segmentation of two objects can be regarded as a classification problem.

Consequently, the result can be measured as the probabilities of correct classification P_c and false classification P_f, which are defined by:

$$P_c = \frac{N_{1c}}{N_{1r}} \quad (22)$$

$$P_f = \frac{N_{1f}}{N_{2r}} \quad (23)$$

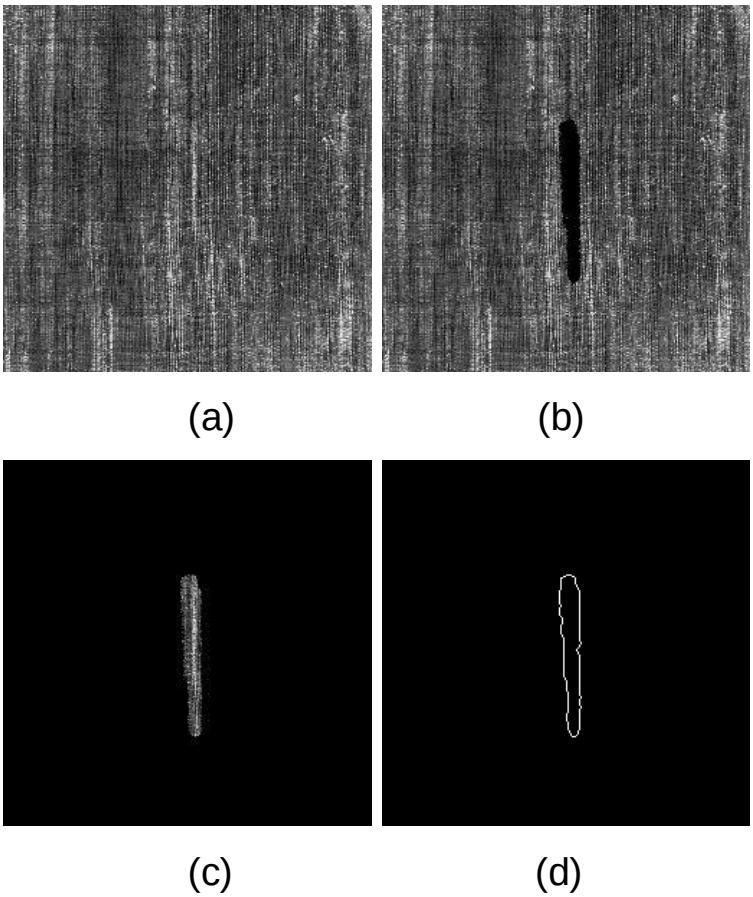

Figure 14. The acquisition of reference edge pixels, (a) original image, (b) original image (c) ground truth image, (d) the reference edge pixels.

where N_{1r} and N_{2r} is the number of pixel in the reference R_1 and R_2, respectively. N_{1c} is the number of detected pixels which are correct relative with R_1. N_{1f} is the number of pixels which belong to (R_2) and incorrectly classified in R_1. These criteria were employed by Dou et al., (2005), to evaluate the effectiveness of the segmentation method in the case of abnormal tissue.

In our application, these criteria are used to evaluate the segmentation method in the case of defects detection in the textured images.

The performance of the proposed method is quite acceptable. In fact, one can observe in Figures 15(c), 15(d), 15(e) and 15(f) that 61.97, 67.78, 65.14 and 61.87% of pixels were correctly segmented for the Prewitt, Canny, Sobel and Laplacian edge detectors, respectively, but, the correctly segmented pixels are increased by our proposed method (77.86%).

However, this demonstrates that the simple edge detectors are unstable in noisy environments and provides edges normally discontinuous or badly detected. However, errors were largely reduced when exploiting simultaneously the statistical features and thresholding techniques.

Comparing Figures 15(c), 15(d), 15(e) and 15(f) with (g), we can see that the signal corresponding to the defect resulting from the proposed method is much detected than the one resulting from the Prewitt, Canny, Sobel and Laplacian edge detectors.

Indeed, only 13.19% of pixels were incorrectly classified in Figure 15(g). This good performance between these methods can also be easily assessed by visually comparing the segmentation results.

These observations are also confirmed by observing the probability of correct and false detection presented respectively in Tables 2 and 3.

In Table 2, one can observe in the figure number 5 of the Data set used in the experiment, the probability of correct classification obtained by our technique (77.86%) is higher than those obtained by the Prewitt (61.97%), Canny (67.78%), Sobel (65.14%) and Laplacian (61.87%) edge detectors. Its indicator corresponding to Pf% (11%) is also lower than the other edge detectors.

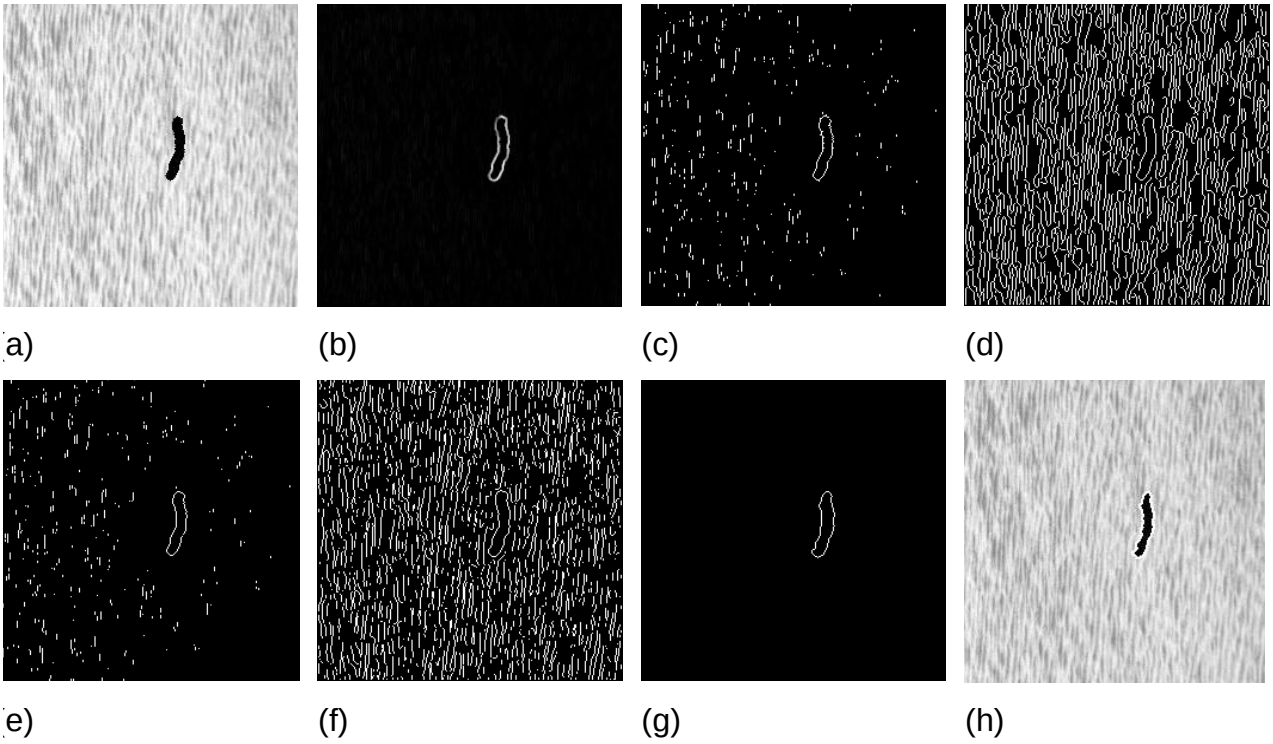

Figure 15. Defect localization in textured image, (a) original image, (b) variance image, (c) edges obtained by the Prewitt operator, (d) edges obtained by the Canny operator, (e) edges obtained by the Sobel operator, (f) edges obtained by the Laplacian operator, (g) edges obtained by the proposed technique, and (h) Defect localization obtained by the proposed technique.

Table 2. Probability of correct classification from the Prewitt, Canny, Sobel, Laplacian operators, and the proposed technique for the data set shown in Figure 13.

Classification	Probability of correct classification				
	Prewitt operator	Canny operator	Sobel operator	Laplacian operator	Proposed technique
Image 4	0.6074	0.6196	0.5951	0.5656	0.7117
Image 5	0.6197	0.6778	0.6514	0.6187	0.7786
Image 6	0.6595	0.7081	0.6801	0.6434	0.8141
Image 7	0.7735	0.7805	0.7497	0.7125	0.8973
Image 8	0.6855	0.7360	0.7072	0.6455	0.8464
Image 9	0.5790	0.6159	0.5863	0.5622	0.7081
Image 10	0.7592	0.7676	0.7303	0.7107	0.8979
Image 11	0.6009	0.6392	0.6081	0.5835	0.7441
Image 12	0.6892	0.7331	0.6975	0.6692	0.8027

Consequently, the experimental results indicate that the proposed method, which combines the statistical features and the thresholding technique, is more accurate than the traditional methods in terms of segmentation quality as denoted by the probability of correct and false classification (Tables 2 and 3).

Conclusion

The segmentation approach proposed in this paper, is conceptually different and explores a new strategy; in fact, instead of considering an elaborate and better designed segmentation model of natural and textured

Table 3. Probability of false classification from the Prewitt, Canny, Sobel, Laplacian operators, and the proposed technique for the data set shown in Figure 13.

Classification	Probability of false classification				
	Prewitt operator	Canny operator	Sobel operator	Laplacian operator	Proposed technique
Image 4	0.35	0.35	0.36	0.43	0.11
Image 5	0.33	0.33	0.34	0.41	0.13
Image 6	0.29	0.28	0.32	0.36	0.27
Image 7	0.17	0.16	0.19	0.21	0.14
Image 8	0.26	0.25	0.26	0.27	0.21
Image 9	0.38	0.37	0.39	0.39	0.17
Image 10	0.18	0.18	0.18	0.19	0.15
Image 11	0.35	0.34	0.35	0.36	0.19
Image 12	0.26	0.25	0.27	0.27	0.21

images, our technique rather explores the possible alternative of combining two segmentation techniques in order to get a good consistency edges.

The obtained results showed the generic and robust character of the approach in the sense that the spatial neighborhood information is introduced to take account the spatial correlation between neighboring pixels that exists in any physical images. The obtained results demonstrate the significantly improved performance in segmentation.

Generally, classical edge detection method has great limitation, because the noise contained in the image has significant influence on the results, while the speed of edge detection and whether the edge can be detected or not are also the concerned problems. This paper proposed a new edge detection method based on the statistical features and automatic thresholding, which can accurately detect the edges and suppress the impact of the noise on the results, while the edge has a good consistency. Extensive testing results have shown great potential on our novel method.

REFERENCES

Ben Chaabane S, Sayadi M, Fnaiech F, Brassart E (2010). Colour Image Segmentation using Homogeneity approach and Data Fusion Techniques. Eurasip J. Adv. Sig. Process. 1155:1-11.

Ben Mhammed I, Abid S, Fnaiech F (2012). Weld defect detection using a modified anisotropic diffusion model. Eurasip J. Adv. Sig. Process. 46:1-12.

Chao SM, Tsai DM (2008). An anisotropic diffusion-based defect detection for low-contrast glass substrates. Image Vis. Comput. 26:187-200.

Colot O, Devinoy R, Sombo A, Brucq D (1998). A Colour Image Processing Method for Melanoma Detection. Lect. Notes Comp. Science, Springer, Berlin 1496:562-569.

Davis L (1975). Survey of edge detection techniques. Computer vision. Graph Image Process. 4:248-270.

Dou W, Ren Y, Chen Y, Ruan S, Bloyet D, Constans JM (2005). Histogram-based Generation Method of Membership Function for Extracting Features of Brain Tissues on MRI Images. Lect. Notes Comp. Sci. Artif. Intell. (LNCS/LNAI). 3613:189-194.

Duda RO, Hart PE, Sork DG (2000). Pattern Classification. Wiley-Interscience, New York, NY, USA 2000:1-654.

Fan J, Wang R, Zhang L, Xing D, Gan F (1996). Image sequence segmentation based on 2-D temporal entropy. Patt. Recognit. Lett. 17(10):1101-1107.

Fan J, Zhang L, Gan F (1997). Spatiotemporal segmentation based on spatiotemporal entropic thresholding. Opt. Eng. 36(10):2845-2851.

Grau V, Mewes AU, Alcaniz M, Kikinis R, Warfield SK (2004). Improved watershed transform for medical image segmentation using prior information. IEEE Trans. Med. Imag. 23(4):447-458.

Haralick RM, Shanmugan K, Distein I (1973). Textural features for image classification. IEEE Trans. Syst. 3:610-621.

Hildreth E (1980). Theory of edge detection. Proc. R. Soc. Lond. 207:187-217.

Hum YC, Teng JB, Lai KW, Tan TS, Sh-Hussain S (2011). Performance metrics for active contour models in image segmentation. Int. J. Phys. Sci. 6(27):6329-6341.

Jianping F, David K, Yau Y, Ahmed KE, Walid GA (2001). Automatic Image Segmentation by Integrating Color-Edge Extraction and Seeded Region Growing. IEEE Trans. Image Process. 10(10):1454-1466.

Liu G, Haralick RM (2000).Assignment problem in edge detection performance evaluation. IEEE Proc. Comput. Soc. Conf. Comput. Vision Patt. Recognit. 1:26-31.

Mery D, Berti MA (2002). Automatic flaw detection in aluminum castings based on the tracking of potential defects in a radioscopic image sequence. IEEE Trans. Robot. Autom. 18(6):890-901.

Nacereddine N, Zelmat M, Belaifa SS, Tridi M (2005). Weld defect detection in industrial radiography based digital image processing. Proc. World Acad. Sci. Eng. Technol. 2:1-10.

Nalwa VS, Binford TO (1986). On detecting edges. IEEE Trans. Patt. Anal. Machine Intell. 8(6):699-714.

Poggio T (1979). A computational theory of human stero vision. Proc. R. Soc. Lond. B. 204:301-328.

Prewitt J (1970). Object enhancement and extraction. Picture Process Psychopict. 1970:75-149.

Qian RJ, Huang TS (1996). Optimal edge detection in two-dimensional images. IEEE Trans. Image Process. 5(7):1215-1220.

Rodriguez R, Suarez AG (2006). A new algorithm for image segmentation by using iteratively the mean shift filtering. Sci. Res. Essay 1(2):43-48.

Shih FY, Cheng S (2005). Automatic seeded region growing for color image segmentation. Image Vision Comput. 23(10):877-886.

Van GW, Scheunders P, VanDyck D (1999). Statistical texture characterisation from discrete wavelet representation. IEEE Trans. Image Process. 8(4):592-598.

Yang Y, Zheng C, Lin P (2005). Fuzzy C-means clustering algorithm with a novel penalty term for image segmentation. Op. Elect. Rev. 13(4):309-315.